J. Mech. Phys. Solids Vol. 37, No. 6, pp. 673–691, 1989.
Printed in Great Britain.

0022-5096/89 $3.00 + 0.00

CRACK TIP SINGULAR FIELDS IN DUCTILE CRYSTALS WITH TAYLOR POWER-LAW HARDENING. II: PLANE STRAIN

MARYAM SAEEDVAFA and JAMES R. RICE

Division of Applied Sciences, Harvard University, Cambridge, MA 02138, U.S.A.

(*Received* 2 *August* 1988)

ABSTRACT

AN ASYMPTOTIC singular solution of the HRR type is presented for mode I tensile cracks in ductile single crystals. These are assumed to undergo Taylor hardening with a power-law relation between stress and strain at sufficiently large strain. Results are given for a crack on the (010) plane with its tip along the $[10\bar{1}]$ direction, and for a crack on the (101) plane with its tip along the same $[10\bar{1}]$ direction in a fcc crystal. The yield surfaces for both of these orientations are identical and thus, for the "small strain" formulation, the same macroscopic solution applies to both. The near-tip region is divided into angular sectors which are maps of successive flat segments and vertices of the yield surface. While the solution here involves 14 different sectors referring to stress states corresponding to flat and vertex segments of the yield locus, RICE's (*Mech. Mater.* **6**, 714, 1987) asymptotic solution for the elastic–ideally plastic crystals involved only 7 sectors which mapped into the vertex points of the yield surface. The perfectly plastic limit of the HRR fields here reduce to 7 stress states of RICE (1987). In this limit, the HRR displacement fields remain continuous resulting in a discontinuous yet bounded and nonzero strain field. In contrast, the elastic–ideally plastic solutions have discontinuous shear displacements across sector boundaries. Furthermore the contours of constant effective strain here have various peaks and troughs at sector boundaries and lean backward relative to the direction of crack growth. Conversely, in the recent finite element solutions for elastic–ideally plastic single crystals by Hawk (preliminary summary of results is included in RICE *et al.*, *Int. J. Fracture*, in press, 1989), the plastic zones lean forward and the strain field is consistent with a Dirac singular form similar to RICE's (1987). Thus it is conjectured that, similar to the anti-plane shear case of RICE and SAEEDVAFA (*J. Mech. Phys. Solids* **36**, 189, 1988), the single crystal HRR fields are dominant only over part of the plastic region immediately adjacent to the crack tip, and that their domain of validity vanishes as the perfectly plastic limit is approached.

INTRODUCTION

RICE (1987) presented an asymptotic solution for the stress and deformation field very near the tip of a mode I crack in an ideally plastic ductile crystal. Two specific orientations, a crack on the (010) cube face with its tip along the $[10\bar{1}]$ face diagonal and a crack on the (101) plane with its tip along the same diagonal, were considered in fcc and bcc crystals for both stationary and quasi-statically growing cracks. In the case of stationary cracks, the stress field was found to be piecewise constant in angular sectors mapping into vertex points of the yield surface and changed discontinuously between sectors. The displacement and strain fields were not fully determined, although it was shown that there must be a shear displacement discontinuity across the sector boundaries for elastic–plastic crystals. The full solution could only be

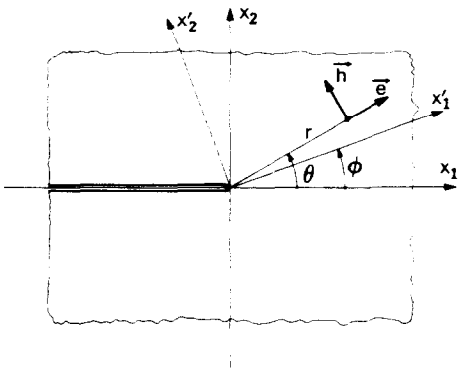

FIG. 1. Coordinate system used.

obtained with the aid of a complete elastic–plastic analysis, recently obtained by Hawk (see RICE *et al.*, 1989) by finite element methods.

In this paper, a solution of the HRR type for the near-tip field of tensile loaded cracks in strain hardening single crystals is presented, with the assumption that there is a power-law relation between stress and strain. The analogous anti-plane shear case was presented in Part I (RICE and SAEEDVAFA, 1988). The general form of the solution governing the field is derived, and is applied to the same two cases of RICE (1987) for stationary cracks in fcc crystals. The present solution procedure may be applied to any other crack and crystal orientation compatible with plane strain deformation through proper choice of parameter sets related to that orientation when assembling the sectors.

MATHEMATICAL FORMULATION

A Cartesian coordinate system fixed with the crack tip is used, as shown in Fig. 1. The polar coordinates r and θ have associated unit vectors **e** and **h**, in the radial and angular directions, respectively. Also,

$$\partial r/\partial x_\gamma = e_\gamma, \quad \partial\theta/\partial x_\gamma = h_\gamma/r \tag{1}$$

govern the transformation to polar coordinates. Conventional index notation is used here where repeated indices imply summation. Greek indices $\alpha, \beta, \ldots$ range over 1 and 2, while latin indices $i, j, \ldots$ have the values of 1, 2 and 3. The crack and crystal orientations considered, and the method of loading, are such that plane strain is a possible deformation state. That is, $\varepsilon_{33} = \varepsilon_{32} = \varepsilon_{31} = 0$ and $u_1 = u_1(x_1, x_2)$, and $u_2 = u_2(x_1, x_2)$. The non-vanishing stresses are of the type $\sigma_{\alpha\beta}$ and σ_{33} only. It may be assumed that the same plane strain singularity (to be discussed later), applies also to general 3-D crack problems so long as ε_{3j} is bounded at the crack front.

Coordinate rotations will be used to simplify the derivation. For a counter-clockwise rotation by an angle ϕ, as in Fig. 1, vector transformation is governed by the rule

$$x_1 + \mathrm{i}x_2 = \mathrm{e}^{\mathrm{i}\phi}(x_1' + \mathrm{i}x_2'), \tag{2}$$

where $i = \sqrt{-1}$. The transformation of stresses is then governed by

$$(\sigma_{22}-\sigma_{11})/2+i\sigma_{12} = e^{2i\varphi}[(\sigma'_{22}-\sigma'_{11})/2+i\sigma'_{12}], \tag{3}$$

with $\sigma_{11}+\sigma_{22} = \sigma'_{11}+\sigma'_{22}$.

It is assumed that the crystals deform by shear on a set of allowable slip systems according to the Schmid rule. That is, plastic flow occurs on a given system only when the resolved shear stress on that system reaches a critical value, which evolves with ongoing deformation. In addition, the critical shear strengths are assumed here to obey Taylor hardening (all systems harden equally) with a power-law relation between stress and strain at sufficiently large strain. That is,

$$\gamma = a\tau^n, \tag{4}$$

where a is the hardening constant and n is the hardening exponent; $n \to \infty$ is the perfectly plastic limit. In the above equation γ is the effective shear strain, as defined in RICE and SAEEDVAFA (1988) (i.e. the sum of absolute shears on all slip systems) and τ is the (common) critical resolved shear stress.

As discussed by RICE (1973), the yield surfaces for plane strain deformation of an incompressible rigid-plastic material satisfying an associated flow rule (as for crystals following the Schmid rule) can be represented as a curve in a plane whose axes are $(\sigma_{11}-\sigma_{22})/2$ and σ_{12}. For the single crystals, the yield surface in this stress space, being the inner envelope of the planar yield surfaces for individual slip systems or groups of systems compatible with plane flow, reduces to a polygon. It is a self-similar polygon for Taylor hardening, and a fixed polygon in the space of the ratio of the stresses to the critical resolved shear stress τ. The yield surface for an elastic–plastic crystal in plane strain may, but need not, have the form of a curve in the $(\sigma_{11}-\sigma_{22})/2$ and σ_{12} plane. That is, there may be a dependence on $\sigma_{11}+\sigma_{22}$ in activating certain secondary slip systems which do not contribute to large plane deformation. The effective yield surface for large plastic straining (similar to the "latent extremal surface" of HILL, 1967) will reduce to a polygon in $(\sigma_{11}-\sigma_{22})/2$ and σ_{12} plane. Such a yield surface is assumed here.

The polygonality of the yield surface results in two different types of near-crack-tip solution associated with stress states corresponding to either a flat segment or a vertex point of the surface. As the yield surface is traversed, the angular range near the crack tip will be divided into sectors corresponding to these possible stress states.

The above constitutive description is compatible with the maximum plastic work inequality and thus involves an associated flow rule. For proportional stressing, the plastic strain vector will be normal to the yield surface along a flat segment and within the cone of limiting normals at a vertex. In the near-tip field, it is anticipated that the elastic strains are relatively small and ignorable. Hence the entire strain tensor can be identified with the plastic strains. Then, the vector with components $(\varepsilon_{11}-\varepsilon_{22})/2$ and ε_{12} based on the entire strain, will be directed normal to the yield locus, in the $(\sigma_{11}-\sigma_{22})/2$ and σ_{12} plane, along flat segments, and within the fan of limiting normals at a vertex. It is assumed that the entire near tip field responds plastically.

For mode I, the only non-trivial equations of equilibrium are

$$\partial\sigma_{\alpha\beta}/\partial x_\alpha = 0. \tag{5}$$

The strains have their usual definition, given by

$$\varepsilon_{\alpha\beta} = (\partial u_\alpha/\partial x_\beta + \partial u_\beta/\partial x_\alpha)/2. \tag{6}$$

Since elastic responses are ignored, the entire material will be incompressible and thus

$$\varepsilon_{\alpha\alpha} = 0. \tag{7}$$

RICE and SAEEDVAFA (1988) have shown that for proportional stressing and straining (as with the HRR singular fields to be discussed later)

$$\tau\gamma = \sigma_{ij}\varepsilon_{ij}. \tag{8}$$

The plastic material described responds identically, under proportional stressing, as a nonlinear elastic material. For power-law hardening plastic material, in which proportional stress states of a type indistinguishable from those for the analogous nonlinear elastic solid are possible, the stress and displacement gradients near the crack tip must be such that the J-integral is path independent. Hence, when evaluated over a circular path surrounding the tip, it is independent of r. As discussed by HUTCHINSON (1968) and RICE and ROSENGREN (1968), this type of field (referred to as HRR) may therefore have singular near-tip stresses, strains and displacements of the form

$$\begin{aligned} \sigma_{ij} &= r^{-1/(n+1)}\hat{\sigma}_{ij}(\theta), \\ \varepsilon_{ij} &= r^{-n/(n+1)}\hat{\varepsilon}_{ij}(\theta), \\ u_i &= r^{+1/(n+1)}\hat{u}_i(\theta), \end{aligned} \tag{9}$$

if singular solutions of the type $u \sim r^\lambda$ exist as $r \to 0$.

By using J-integral type considerations and related conservation laws, RICE (1988) derived two general integrals which apply to all crack tip singular fields in nonlinear elastic materials (as well as in the plastic materials discussed above, since they are responding with proportional stressing and straining). This was also mentioned in RICE and SAEEDVAFA (1988), who noted that therefore for all HRR type fields

$$h_\alpha\sigma_{\alpha\beta}u_\beta = (n+1)C_2 e_2 = (n+1)C_2 \sin\theta, \tag{10}$$

where C_2 is a constant having the same units as the J-integral. In the work that follows, the derivation of the form of the near-tip solution in each of the several angular sectors is greatly simplified by (10), since C_2 is the same in all sectors. In the examples here C_2 will be expressed in terms of J when the field is normalized via the crack tip J-integral, which is expected to be close to the far-field value of J in cases for which the "deformation" plasticity formulation is appropriate.

FLAT SECTORS

Consider an angular sector of points near the tip whose stress state corresponds to a particular flat segment of the (fixed) yield surface in the $(\sigma_{11}-\sigma_{12})/2\tau$ and σ_{12}/τ

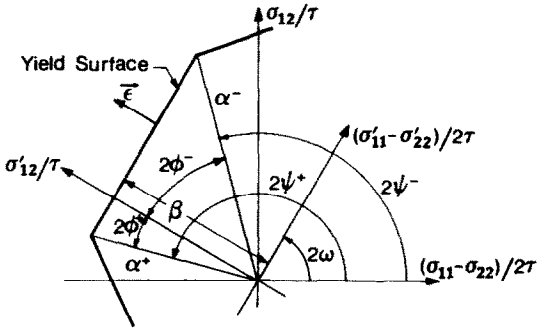

FIG. 2. Notation used for the flat segment of the yield surface.

plane. Since the HRR field (9) involves ratios of stresses to one another that are independent of r, each radial ray corresponds to a particular point of this flat segment. The normality rule requires the strain vector to be perpendicular to that segment as shown in Fig. 2. Thus, rotating the axes by an angle 2ω such that the σ'_{12}/τ axis is perpendicular to the segment (corresponding to a rotation of x_1, x_2 axes by ω) yields $\varepsilon'_{11}-\varepsilon'_{22}=0$. Then, recalling incompressibility of the plastic material, $\varepsilon'_{11}+\varepsilon'_{22}=0$, gives

$$\varepsilon'_{11} = \partial u'_1/\partial x'_1 = 0,$$
$$\varepsilon'_{22} = \partial u'_2/\partial x'_2 = 0. \tag{11}$$

The above equations imply that $u'_1 = u'_1(x'_2)$ and $u'_2 = u'_2(x'_1)$. For HRR fields the displacements vary as $r^{1/(n+1)}$. Since $x'_1 = r\cos(\theta-\omega)$ and $x'_2 = r\sin(\theta-\omega)$,

$$u'_1 = B_1 x'_2 |x'_2|^{-n/(n+1)},$$
$$u'_2 = B_2 x'_1 |x'_1|^{-n/(n+1)}, \tag{12}$$

where B_1 and B_2 are constants. Differentiating (12) yields

$$\varepsilon'_{12} = (u'_1/x'_2 + u'_2/x'_1)/2(n+1). \tag{13}$$

As indicated in Fig. 2, for the flat segment of the yield surface,

$$\sigma'_{12}/\tau = \beta, \tag{14}$$

where β is a constant (≥ 1) depending on the geometrical orientation of the slip system or group of systems corresponding to the flat segment (see RICE, 1987). Since by (8) $\gamma\tau = \sigma_{ij}\varepsilon_{ij} = 2\sigma'_{12}\varepsilon'_{12}$, applying (14) yields

$$\gamma = 2\beta\varepsilon'_{12} \tag{15}$$

and (4) defines τ.

The equilibrium equations (5) may be represented in the integral form as

$$\sigma'_{11} = -\int^{x'_1} \frac{\partial}{\partial x'_2}\sigma'_{12}(\bar{x}'_1, x'_2)\,\mathrm{d}\bar{x}'_1 + f(x'_2),$$

$$\sigma'_{22} = -\int^{x'_2} \frac{\partial}{\partial x'_1}\sigma'_{12}(\bar{x}'_1, x'_2)\,\mathrm{d}\bar{x}'_2 + g(x'_1),$$

where σ'_{12} is defined by (14). For HRR fields, stresses vary as $r^{-1/(n+1)}$. Therefore, since $x'_1 = r\cos(\theta-\omega)$ and $x'_2 = r\sin(\theta-\omega)$, the last terms in the above equations must be a constant multiple of $|x'_2|^{-1/(n+1)}$ and $|x'_1|^{-1/(n+1)}$, respectively; in particular, $f(x'_2) = B_3|x'_2|^{n/(n+1)}/x'_2$ and $g(x'_1) = B_4|x'_1|^{n/(n+1)}/x'_1$. The integrals in the above equation have the form $\partial I/\partial y$, where I is defined as

$$I = \int^{x} [A|y|^{-n/(n+1)} + B|\bar{x}|^{-n/(n+1)}]^{1/n}\,\mathrm{d}\bar{x}$$

$$= \frac{x}{A|x|}|y|^{-1/(n+1)}[A|x|^{n/(n+1)} + B|y|^{n/(n+1)}]^{(n+1)/n}. \tag{16}$$

Carrying out the differentiation yields

$$\frac{\partial I}{\partial y} = \frac{1}{(n+1)}[A|y|^{-n/(n+1)} + B|x|^{-n/(n+1)}]^{1/n}\left[n\frac{B}{A}\frac{x}{y}\left|\frac{x}{y}\right|^{-n/(n+1)} - \frac{x}{y}\right]. \tag{17}$$

After some manipulation, it is obtained that

$$\sigma'_{11} = -\frac{\sigma'_{12}}{(n+1)}(mu'_2/u'_1 - x'_1/x'_2) + B_3B_1/u'_1,$$

$$\sigma'_{22} = -\frac{\sigma'_{12}}{(n+1)}(mu'_1/u'_2 - x'_2/x'_1) + B_4B_2/u'_2. \tag{18}$$

Note that in this sector x'_1 and x'_2 cannot change sign if there are to be finite stresses at $r \neq 0$. This restricts possible boundary locations for the sector. Using the general integral (10) in the transformed coordinate system, the following relations beween the constants of this sector are obtained.

$$B_1B_3 = -(n+1)C_2\cos\omega,$$
$$B_2B_4 = +(n+1)C_2\sin\omega. \tag{19}$$

Sector limits

Since the flat sector of the yield locus is bounded by two vertices, the range of applicability of (11) to (19) is confined to

$$-\tan 2\phi^- \leqslant \frac{(\sigma'_{11}-\sigma'_{22})}{2\sigma'_{12}} \leqslant \tan 2\phi^+,$$

where $2\phi^+ = 2\omega - 2\psi^+ + \pi/2$ and $2\phi^- = 2\psi^- - 2\omega - \pi/2$, as shown in Fig. 2. Simplifying the above equation yields

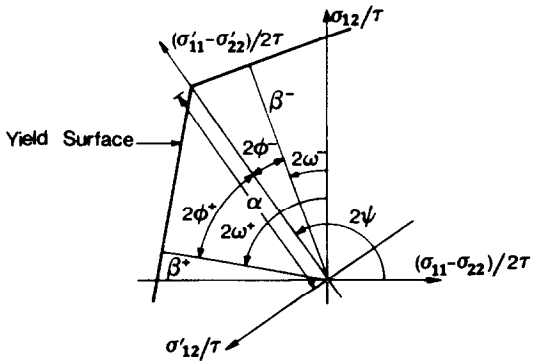

FIG. 3. Notation used for the vertex segment of the yield surface.

$$\cot 2(\omega-\psi^-) \leqslant \frac{(\sigma'_{22}-\sigma'_{11})}{2\sigma'_{12}} \leqslant \cot 2(\omega-\psi^+). \tag{20}$$

Equation (20) indicates that the flat sector starts (or ends) at $\theta = \theta^F$, given by

$$\left[\frac{(\sigma'_{22}-\sigma'_{11})}{2\sigma'_{12}}\right]_{\theta=\theta^F} = \cot 2(\omega-\psi^{\pm}). \tag{21}$$

This is a nonlinear equation for the two values of θ^F (start and end) in terms of the constants of the sector. However, by using (19), this relationship only involves the constants B_1, B_2, which will be determined when assembling the sectors, and C_2, which will be used to normalize the solution with the outer field.

VERTEX SECTORS

For the angular range near the tip which corresponds to the stress state at a vertex of the yield surface, the ratio of stresses to the slip system shear strength τ will remain constant. The orientation of the strain vector changes continuously within the range of the two limiting normals of the flat segments which define the vertex. Using a coordinate system where the $(\sigma'_{11}-\sigma'_{22})/2\tau$ axis passes through the vertex (that is by rotating the x_1, x_2 axes by an angle ψ), as shown in Fig. 3, gives

$$\sigma'_{12} = 0. \tag{22}$$

Then, the equations of equilibrium yield $\partial\sigma'_{11}/\partial x'_1 = 0$ and $\partial\sigma'_{22}/\partial x'_2 = 0$, indicating that $\sigma'_{11} = \sigma'_{11}(x'_2)$ and $\sigma'_{22} = \sigma'_{22}(x'_1)$. Recognizing the special functional form of stress in HRR fields (9), results in

$$\begin{aligned}\sigma'_{11} &= +A_1|x'_2|^{1/(n+1)},\\ \sigma'_{22} &= -A_2|x'_1|^{1/(n+1)},\end{aligned} \tag{23}$$

where A_1 and A_2 are constants. Note that as shown in Fig. 3,

$$\tau = (\sigma'_{11} - \sigma'_{22})/2\alpha, \tag{24}$$

and α can be defined in terms of the constant β and angle ω of either of the neighboring flat sectors as $\alpha = \beta/\sin 2(\psi - \omega)$. Similar to the calculations for the flat sector, using (7) and (8) leads to

$$\varepsilon'_{11} = \partial u'_1/\partial x'_1 = +\gamma/2\alpha,$$
$$\varepsilon'_{22} = \partial u'_2/\partial x'_2 = -\gamma/2\alpha, \tag{25}$$

where γ is given by (4). Equation (25) can be integrated for u'_1 and u'_2 by using (16) after noticing that these integrals have the same form as I if n is replaced by $1/n$. Thus, after some manipulation,

$$u'_1 = \gamma\tau x'_1/\sigma'_{11} + f(x'_2),$$
$$u'_2 = \gamma\tau x'_2/\sigma'_{22} + g(x'_1).$$

For HRR fields the displacements vary as $r^{1/(n+1)}$, thus the last terms of the above equation can be expressed as $f(x'_2) = A_3|x'_2|^{1/(n+1)}$ and $g(x'_2) = -A_4|x'_1|^{1/(n+1)}$, where A_3 and A_4 are constants. Thus,

$$u'_1 = (\gamma\tau x'_1 + A_3A_1)/\sigma'_{11},$$
$$u'_2 = (\gamma\tau x'_2 + A_4A_2)/\sigma'_{22}. \tag{26}$$

Differentiating this for ε'_{12} yields

$$\varepsilon'_{12} = \left\{\frac{\gamma}{2\alpha}\left[\frac{x'_2}{x'_1}\frac{\sigma'_{11}}{\sigma'_{22}} - \frac{x'_1}{x'_2}\frac{\sigma'_{22}}{\sigma'_{11}} - n\left(\frac{x'_1}{x'_2} - \frac{x'_2}{x'_1}\right)\right] + \frac{A_3A_1}{x'_2\sigma'_{11}} + \frac{A_4A_2}{x'_1\sigma'_{22}}\right\}\Big/ 2(n+1). \tag{27}$$

Note that here x'_1 and x'_2 must have the same sign through the whole domain of validity or else unbounded stresses will be encountered at $r \neq 0$. Application of the general integral (10) leads to

$$A_1A_3 = -(n+1)C_2\cos\psi,$$
$$A_2A_4 = +(n+1)C_2\sin\psi. \tag{28}$$

Sector limits

The vertex sector is adjoined by two flat sectors. Therefore, the orientation of the strain vector is restricted to

$$-\tan 2\phi^- \leqslant \frac{\varepsilon'_{12}}{(\varepsilon'_{11} - \varepsilon'_{22})/2} \leqslant \tan 2\phi^+,$$

where $2\phi^+$ and $2\phi^-$ are defined in Fig. 3 as $2\phi^+ = 2\omega^+ - 2\psi - 3\pi/2$, and $2\phi^- = 2\psi - 2\omega^- + 3\pi/2$. Using (25) in the above gives

$$\cot 2(\psi - \omega^-) \leqslant \frac{2\alpha\varepsilon'_{12}}{\gamma} \leqslant \cot 2(\psi - \omega^+). \tag{29}$$

Equation (29) indicates that the vertex sector starts (or ends) at $\theta = \theta^V$, given by

$$\left[\frac{2\alpha\varepsilon'_{12}}{\gamma}\right]_{\theta=\theta^V} = \cot 2(\psi-\omega^{\pm}). \tag{30}$$

Similar to (21), the above is a nonlinear equation for the two angles θ^V in terms of the constants A_1, A_2 and C_2.

Assuming that all components of stress and displacement are continuous (only $h_\alpha\sigma_{\alpha\beta}$ and $h_\alpha u_\alpha$ need to be on *a priori* grounds, and neither $e_\alpha\sigma_{\alpha\beta}e_\beta$ nor $e_\alpha u_\alpha$ are continuous in RICE's (1987) ideally plastic solution), it can be proven, as will be shown later, that (21) and (30) are identical. This implies that there is no gap or overlap between the range of the applicability of the two sector types. Thus, once the constants associated with a sector are known the pertinent one of (21) or (30) may be used to obtain the boundary angle between two adjoining sectors. As mentioned earlier both equations are nonlinear. They can only be solved numerically.

ASSEMBLY OF SECTORS

The general solution of the near-tip field in the preceding sections involves two unknown constants (A_1 and A_2 for the vertex sectors, and B_1 and B_2 for the flat segments) per sector, in addition to the universal (same for all sectors) constant C_2 which is left undetermined for normalization with the outer field. The third set of unknown variables are the boundary angles between the sectors.

The crack free surface boundary conditions are

$$\sigma_{12} = 0 \quad \text{at} \quad \theta = \pi, \tag{31a}$$

$$\sigma_{22} = 0 \quad \text{at} \quad \theta = \pi, \tag{31b}$$

and since the field is symmetric (tensile, or mode I, conditions)

$$\sigma_{12} = 0 \quad \text{at} \quad \theta = 0, \tag{32a}$$

$$u_2 = 0 \quad \text{at} \quad \theta = 0. \tag{32b}$$

For a continuous field the stresses σ_{11}, σ_{22} and σ_{12}, and the displacements u_1 and u_2 must be continuous across sector boundaries. This accounts for five continuity conditions that must be satisfied per sector, in addition to the above four boundary conditions. Also, there are the two equations (21) and (30) which determine the range of applicability of each sector. However there are only three unknown constants per sector. In spite of this the formulation is not too restrictive. There are several redundancies associated with use of the general integral (10) in the derivation. First, as discussed by RICE (1988), the general integral (10) and a related general integral, not given here, can be regarded as the equivalent of two of the governing equations. Furthermore, as examples of the redundancy, at $\theta = 0$ or π, (10) reduces to

$$\sigma_{12}u_1 + \sigma_{22}u_2 = 0.$$

Then, once (31a) is used, (31b) follows automatically provided that on the crack surfaces u_2, the crack opening displacement, does not vanish. Also, presuming that the tensile stress σ_{22} is not zero ahead of the crack, (32a) automatically satisfies

(32b). Moreover, using the continuity of two of the stresses, to determine the two unknowns of the next and (21), to find the boundary angle between these two sectors, the continuity of the third stress is automatically satisfied. Across sector boundaries, (10) reduces to the continuity of $h_\alpha \sigma_{\alpha\beta} u_\beta$, which in the context of continuity of stresses ensures the continuity of displacements. For this power-law hardening material, the continuity of displacements together with the continuity of stresses ensures the continuity of strains. As a result (30) is automatically satisfied. Also using the continuity of the two displacements, to determine the two unknowns of the next flat sector, and (30), to find the boundary angle between these two sectors, together with (10) results in the continuity of strains and stresses. As a result (21) will be automatically satisfied. This means that any two convenient continuity conditions could be used to find the two constants of the next sector. The pertinent one of (21) and (30) may be used to determine the boundary angle. All other continuity conditions will be then automatically satisfied. This leaves only (31a) and (32a) which are used to determine the constants of the first sector.

Since both (21) and (30) involve the constant C_2 and a in a nonlinear form, the field variables are normalized as

$$\begin{aligned} \sigma_{ij} &= [(n+1)C_2/ar]^{1/(n+1)}\bar{\sigma}_{ij}, \\ \varepsilon_{ij} &= a^{1/(n+1)}[(n+1)C_2/r]^{n/(n+1)}\bar{\varepsilon}_{ij}, \\ u_i &= (ar)^{1/(n+1)}[(n+1)C_2]^{n/(n+1)}\bar{u}_i. \end{aligned} \tag{33}$$

Then defining

$$\bar{B}_\alpha = B_\alpha a^{-1/(n+1)}[(n+1)C_2]^{-n/(n+1)}, \quad \alpha = 1, 2 \tag{34}$$

for the flat sectors, and

$$\bar{A}_\alpha = A_\alpha[(n+1)C_2/a]^{-1/(n+1)}, \quad \alpha = 1, 2 \tag{35}$$

for the vertex sectors, eliminates C_2 and a in (21) and (30), which now depend only on $\bar{B}_\alpha$ and $\bar{A}_\alpha$, respectively.

So far all the equations are given for a general case. Specific examples involve numerical solution as follows:

(1) Equation (32a) or (32b) is used to obtain the ratio of the constants of the first sector and the value of the second constant is assumed.

(2) Equation (21) or (30) is used ((21) for the flat sectors since (30) was already incorporated into its derivation, and (30) for the vertex sectors since (21) is built into its derivation) to determine the boundary angle.

(3) Any two convenient sets of continuity conditions (e.g. the continuity of the displacements for vertex to flat boundary, and the continuity of the two stresses σ_{11} and σ_{22} for flat to vertex boundary) are used to determine the constants of the next sector.

(4) Items 2 and 3 are repeated until the last sector is reached.

(5) Items 1 through 4 are iterated, by choosing a different value for the second constant of the first sector, until (31a) is satisfied.

TABLE 1

n	3	5	8	20
$\theta_{1'}$	22.220°			
$\theta_{1''}$	34.015°			
θ_1	34.329°	33.289°	32.858°	32.298°
θ_2	57.591°	56.310°	55.609°	54.902°
θ_3	60.403°	57.620°	56.200°	54.942°
θ_4	98.238°	94.891°	92.969°	91.095°
θ_5	108.964°	101.475°	96.885°	92.367°
θ_6	131.385°	129.141°	127.712°	126.221°
C_2/J	0.014290	0.013136	0.010994	0.007036
$\delta(J/ar)^{1/(n+1)}/J$	0.972978	0.831498	0.740982	0.641273

J-INTEGRAL NORMALIZATION

As mentioned earlier the constant C_2 was left free for normalization with the outer field. Such normalization is possible through the J-integral, associated with the near-tip singular field and, to the extent that J is approximately path independent in the actual elastic–plastic material, this is the same as the far field J. Here J is defined as

$$J = \int_{-\pi}^{+\pi} [We_1 - e_\alpha \sigma_{\alpha\beta} \partial u_\beta / \partial x_1] r \, d\theta, \quad \alpha, \beta = 1, 2, \tag{36}$$

where the path for evaluation is taken as a circle of radius r, and W is the strain energy density of the equivalent nonlinear elastic material, defined as

$$W = \int_0^{\varepsilon_{mn}} \sigma_{ij} \, d\varepsilon_{ij} = [n/(n+1)] \sigma_{ij} \varepsilon_{ij} = [n/(n+1)] \gamma\tau. \tag{37}$$

The integral in (36) is the sum of its corresponding values in each sector and can be numerically integrated for each example after assembling the sectors. This leads to $J \propto C_2$, where the constant of proportionality depends only on the geometry of the array of flats and vertices making up the yield locus and on the hardening exponent. Such values are tabulated in Table 1 for the specific examples considered here.

EXAMPLES

As a first example, a crack on the (010) cube-face plane in a fcc crystal, with its tip along the face-diagonal direction $[10\bar{1}]$, is analysed. The crack and crystal orientation are shown in Fig. 4(a). For fcc metal crytals, there are twelve different possible slip systems, consisting of the four $\{111\}$ slip planes with three $\langle 110 \rangle$ slip directions on each system. The resulting yield surface, which is the inner envelope of all the lines of critical shear stress, for all possible systems, in the two-dimensional plane strain stress space is shown in Fig. 5(a). Active members of the $\{111\}$ $\langle 110 \rangle$ type systems are

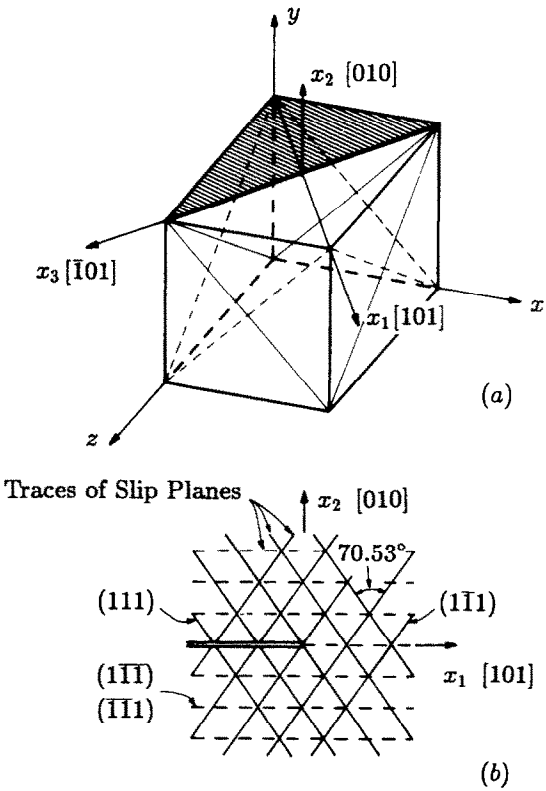

FIG. 4. (a) Fcc crystal with crack on (010) plane and its tip along the $[10\bar{1}]$ direction. (b) Crack in the plane of problem. The solid lines are the intersections of slip planes (111) and $(1\bar{1}1)$ with the $x_3 = 0$ plane. the dashed lines are the traces of simultaneous slip on the two planes $(1\bar{1}\bar{1})$ and $(\bar{1}\bar{1}1)$.

indicated along each line. Figure 4(b) shows the crack in the x_1-x_2 plane. The solid lines in this figure are the intersection of the slip planes (111) and $(1\bar{1}1)$ with the $x_3 = 0$ plane. Simultaneous slip on the two planes $(1\bar{1}\bar{1})$ and $(\bar{1}\bar{1}1)$ will cause an effective slip in the [101] direction which is parallel to the x_1 axis. This results in the horizontal segments of the yield surface in Fig. 5(a) and an effective slip plane trace which is marked with the dashed horizontal lines in Fig. 4(b).

The solution for the orientation of Fig. 4 also provides the solution, within the "small strain" formulation (e.g. neglect of lattice rotation), for a second orientation, which is a crack on the (101) plane with its tip along the same $[10\bar{1}]$ direction. This crack and crystal orientation are shown in Fig. 6(a). Figure 6(b) shows the crack in the deformation plane (x_1 and x_2 plane). Again the solid lines are the intersection of slip planes (111) and $(1\bar{1}1)$ with the $x_3 = 0$ plane and the dashed lines are traces of the effective slip plane formed by simultaneous slip on the two planes $(1\bar{1}\bar{1})$ and $(\bar{1}\bar{1}1)$, which now cause an effective slip parallel to the x_2 axis. The corresponding yield surface is the same as that of the first orientation except that the sign of the slip directions marked in Fig. 5(a) should be reversed. As mentioned by RICE (1987) these two crack orientations are encountered in experimental studies.

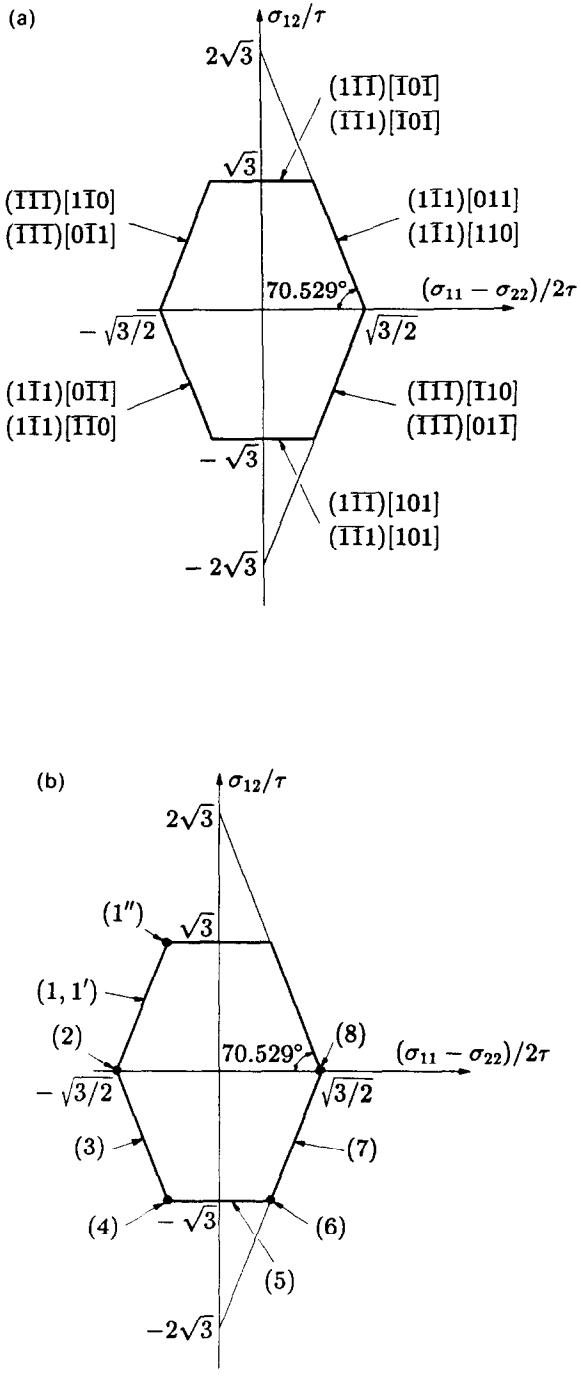

FIG. 5. Yield surface for fcc crystal with crack on (010) plane and its tip along the $[10\bar{1}]$ direction. (a) Active slip planes for this orientation. For the case of the crack on the (101) plane the sign of the slip directions should be changed. (b) Sector arrangement.

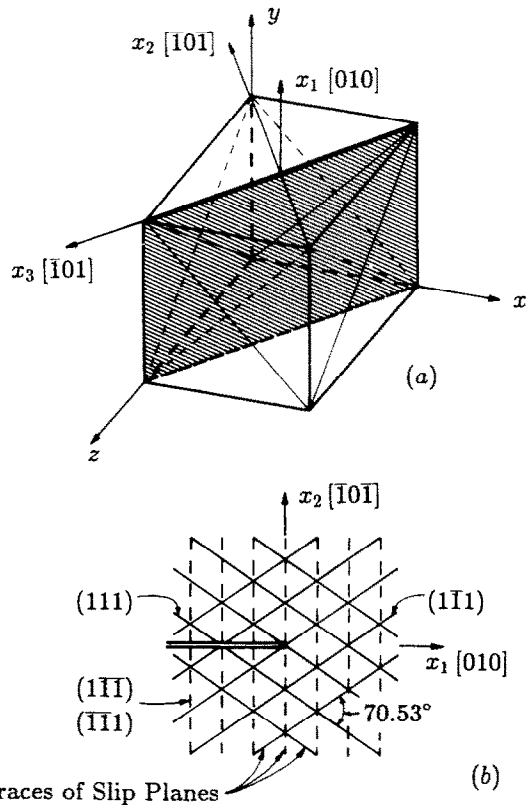

FIG. 6. (a) Fcc crystal with crack on (101) plane and its tip along the [10$\bar{1}$] direction. (b) Crack in the plane of problem. The solid lines are the intersections of slip planes (111) and (1$\bar{1}$1) with the $x_3 = 0$ plane. the dashed lines are the traces of simultaneous slip on the two planes (1$\bar{1}\bar{1}$) and ($\bar{1}\bar{1}$1).

On the crack surfaces the stress $\sigma_{12} = 0$. For a positive mode I loading, it is anticipated that $(\sigma_{11}-\sigma_{22})/2$ is positive on the surfaces of the crack. Thus, a point on the surfaces of the crack should correspond to the vertex point marked (8) on the $(\sigma_{11}-\sigma_{22})/2\tau$ axis in Fig. 5(b). Due to symmetry of the yield surface about the $(\sigma_{11}-\sigma_{22})/2\tau$ axis the field is also symmetric about $\theta = 0$ along which ray $\sigma_{12} = 0$. It is anticipated that $(\sigma_{11}-\sigma_{22})/2$ is negative ahead of the crack (i.e. it is expected that $\sigma_{22} \geqslant \sigma_{11}$ on $\theta = 0$). So a point on the ray $\theta = 0$ should correspond to the vertex point marked (2) in Fig. 5(b). Thus, traversing counter-clockwise around the crack from $\theta = 0$ to π is expected to correspond to going counter-clockwise on the yield surface from point (2) to point (8) of Fig. 5(b) along the yield surface. However as will be explained in the following, the solution does not exactly exhibit this behavior.

Vertex point (2) is not expected to correspond to an angular sector of finite range which contains the ray $\theta = 0$. The only non-zero stress then would be σ_{22}, since $2\psi = \pi$ and $x_1' = r\cos(\theta-\psi) = 0$ at $\theta = 0$, and for finite stresses at $r \neq 0$, $A_2 = 0$ in (23), or $\sigma_{22}' = \sigma_{11} = 0$. This seems to contradict the expected stress triaxiality ahead of the

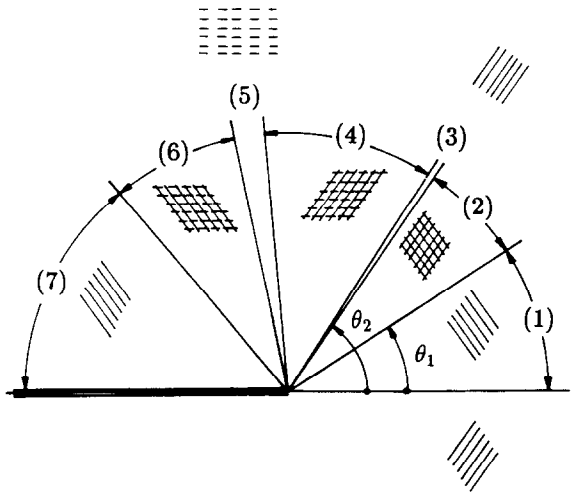

FIG. 7. Sector arrangement in the x_1–x_2 plane. The numbers in parentheses refer to the sectors marked in Fig. 6(b). The active slip plane or planes are marked within each sector for the fcc crystal with a crack on the (010) plane and its tip along the $[10\bar{1}]$ direction. These slip lines should be rotated by 90 for the case of the crack on the (101) plane.

crack and is improbable. But more importantly, a solution constructed this way does not meet the correct boundary condition on the crack surfaces, and thus no such solution exists. Also, vertex (8) is not expected to correspond to an angular sector of finite range including the crack surface since this would result in a zero stress sector there, which is unlikely. The reason that all the stresses would be zero within such a vertex sector is that $\psi = 0$ and $x_2' = r \sin(\theta - \psi) = 0$ at $\theta = \pi$, and for finite stresses at $r \neq 0$, $A_1 = 0$ in (23), or $\sigma_{11}' = \sigma_{11} = 0$. Also the boundary equation (31b) requires $\sigma_{22} = \sigma_{22}' = 0$ at $\theta = \pi$, which means $A_2 = 0$, and for a vertex sector $\sigma_{12}' = \sigma_{12} = 0$. Thus the solution must start at the intersection of one of the flat segments adjoining vertex (2) of Fig. 5(b) with the axis $\sigma_{12} = 0$ at $\theta = 0$, and then move along this flat segment as θ changes from zero, and end at the intersection of one of the flat segments adjoining vertex (8) with $\sigma_{12} = 0$ at $\theta = \pi$.

After many trials, it was found to be impossible to construct a solution which monotonically travels the yield surface counter clockwise as θ increases from 0 to π. Just as was the case for HRR field in isotropic material (e.g. Fig. 9 of RICE and ROSENGREN, 1968), with increasing θ the yield surface is first traversed in the direction of positive σ_{12}. For the single crystals considered here this corresponds to traveling up along flat (1) in Fig. 5(b). The sign of $\partial\sigma_{12}/\partial\theta$ then reverses and the yield surface is traversed counter clockwise toward vertex (8), stopping just at the end of flat (7). The initial rise along line (1), before $\partial\sigma_{12}/\partial\theta$ changes sign, is a function of the hardening exponent n: the smaller n the larger the rise in σ_{12}. For example, for $n = 3$ the rise extends all the way to vertex (1″). The resulting arrangement of angular sectors is shown in Fig. 7, where the corresponding regions are numbered in reference to Fig. 5(b). In this figure, the active slip plane or planes are shown within each sector for the case of the crack on (010) plane of Fig. 4. For the orientation with the crack on

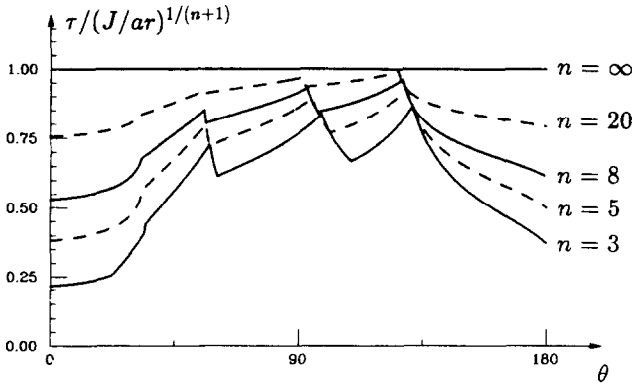

FIG. 8. Angular variation of τ for $n = 3, 5, 8, 20, \infty$.

the (101) plane of Fig. 6, these slip planes should be rotated by 90°, since the x_1–x_2 plane is rotated by 90° with respect to the previous orientation. The boundary angles $\theta_1, \theta_2, \ldots$ are given in Table 1, for various n. In the case of $n = 3$, sector (1) should be divided into three sectors; (1′), (1″) and (1), in order of increasing θ. Table 1 also shows the value of C_2/J and the crack opening displacement $\delta = 2\mu_2(r, \pi)$.

Figure 8 shows the variation of τ with θ. As can be seen in this normalized plot, τ approaches the constant value of $(J/ar)^{1/(n+1)}$ as $n \to \infty$. With the interpretation of a in (4) as $a = \gamma_0 \tau_0^{-n}$ (where the constants γ_0 and τ_0 are the initial yield strain and stress in shear, respectively, or the yield strain and stress as $n \to \infty$) $(J/ar)^{1/(n+1)} \to \tau_0$, or $\tau \to \tau_0$, the ideally plastic yield shear stress.

Figure 9 shows the variation of $(\sigma_{11}+\sigma_{22})/2\tau$ with θ. Figure 10 shows the variation of σ_{12} with θ. As n becomes larger, the already small angular ranges of sectors (3) and (5), indicated in Table 1, become even smaller. As expected these ranges vanish as $n \to \infty$. While the ranges of sectors (1) and (7) remain finite as n becomes large, the entire stress fields of these two sectors correspond to the intersection of the corresponding flat sector with the $(\sigma_{11}-\sigma_{22})/2\tau$ axis (i.e. vertices (2) and (8) of Fig.

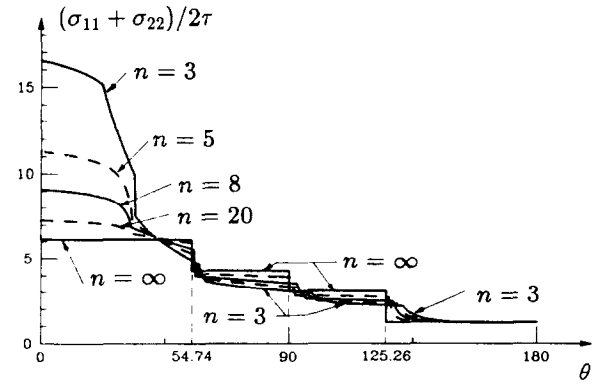

FIG. 9. Angular variation of $(\sigma_{11}+\sigma_{22})/2\tau$ for $n = 3, 5, 8, 20, \infty$.

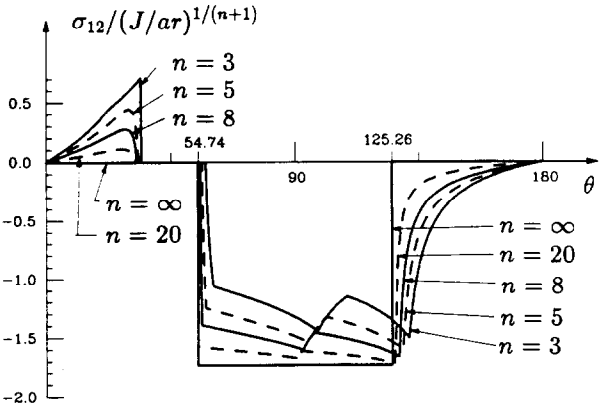

FIG. 10. Angular variation of σ_{12} for $n = 3, 5, 8, 20, \infty$.

5b respectively), as marked by $n = \infty$ curves in Figs 9 and 10. The solution in the limit of large n exhibits the discontinuous stress field of RICE (1987) for the ideally plastic material. In his solution the entire stress field corresponded to jumps from vertex to vertex points of the yield surface [(2), (4), (6) and (8) in that order]. The boundary angles differ from those of the ideally plastic solution (for which two of the angles corresponded to the $\{111\}$ slip plane traces for the first configuration, Fig. 4, and were perpendicular to those traces for the second configuration, Fig. 6) by order of $1/n$ for large n.

Figure 11(a) shows the contour of constant γ for $n = 5$. The contours of constant γ (and thus also τ) exhibit sharp peaks and troughs. They lean backward relative to the direction of cracking, which indicates more straining in that direction. It should be noted that the contour of constant equivalent strain in the isotropic case of RICE and ROSENGREN (1968) also leaned backward, and the equivalent strain was very small at $\theta = 0$ and π (their Figs 3 and 4). As shown in Fig. 11(b), γ is not zero at $\theta = 0$ and π, but becomes of the order of $1/n$ as n becomes large. Furthermore, while γ is not discontinuous, the range of some of the sectors in which it varies significantly is small. At large n the ranges of sectors (3) and (5) become of order $1/n$ and thus γ becomes discontinuous in the ideally plastic limit, $n \to \infty$, but does not approach the Dirac δ-function form of RICE (1987) for the elastic–ideally plastic material, which corresponds to a slip discontinuity of displacements. Note that Rice's proof that the displacements associated with his stress field must (versus may) be discontinuous at sector boundaries assumed finite elastic moduli; it does not apply to rigid plastic materials or to cases like here where the elastic strains are neglected. Figure 12 shows the variation of u_r with θ. The shear displacement remains continuous as $n \to \infty$.

The limiting behavior of HHR fields in mode I is analogous to the anti-plane shear case of RICE and SAEEDVAFA (1988) where the $n \to \infty$ limit had the correct stress discontinuities at the sector boundaries but showed a continuous displacement field and hence, a non-Dirac strain field. In contrast, the RICE and NIKOLIC (1985) complete elastic–ideally plastic solution for mode III stationary cracks showed plastic flow occurring along discrete planes emanating from the tip at sector boundaries across

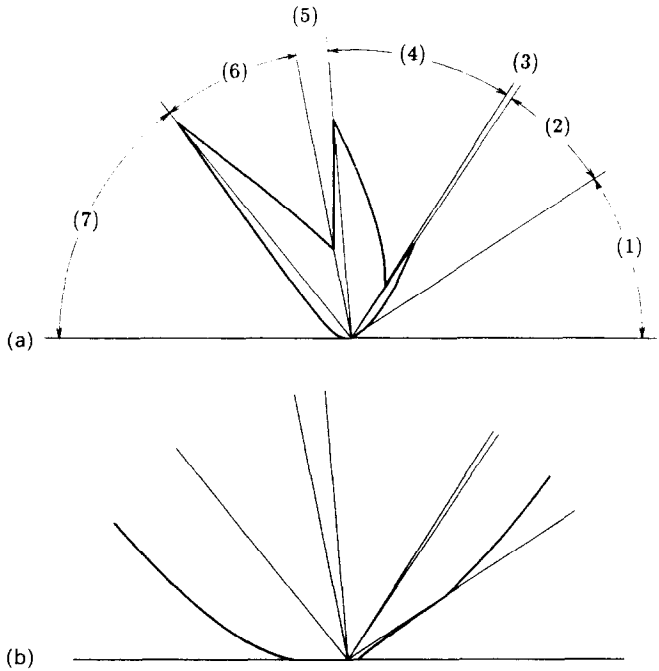

FIG. 11. (a) Contour of constant γ for $n = 5$. (b) Enlargement of details at $\theta = 0, \pi$.

which both the stress and displacements were discontinuous. There, just as is the case with RICE (1987), the asymptotic solution only determined the stress field and allowed a family of solutions for the strain and displacement fields. It was not until the full elastic–plastic analysis was done that the strain field was uniquely determined.

DISCUSSION

It is conjectured that the domain of dominance of the HRR field for single crystals under mode I loading, as well as mode III loading, is limited only to a part of the

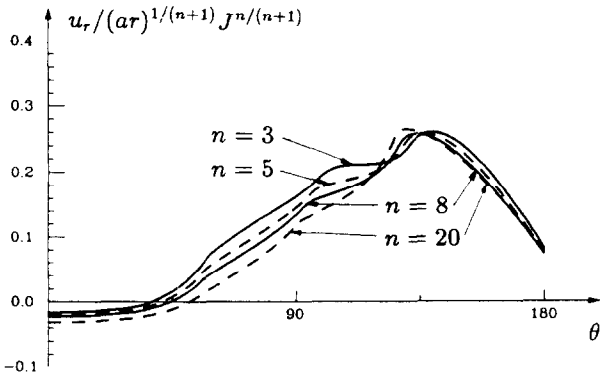

FIG. 12. Angular variation of u_r for $n = 3, 5, 8, 20$.

plastic zone immediately adjacent to the crack tip. As the perfectly plastic limit is approached, this domain must shrink to zero since the HRR solution does not yield the perfectly plastic displacement and strain fields of RICE (1987). The HRR singular field presented here shows a continuous displacement field, while the elastic–perfectly plastic solution of RICE (1987) shows a shear displacement discontinuity across sector boundaries with an associated Dirac singular form for the plastic strain. Furthermore the HRR field contours of constant shear strength and the equivalent shear strain for single crystals lean backward relative to the direction of crack growth and show more straining at the end of sector (6), as shown in Fig. 11. In contrast, in the recent results obtained by the finite element method for elastic–perfectly plastic single crystals with mode I loaded cracks by Hawk (a preliminary summary is given in the review by RICE *et al.*, 1989) the plastic zones are observed to lean forward showing more straining in that direction. His numerical displacement field is consistent with shear displacement discontinuities at the orientations predicted by RICE (1987), and his strain field with a Dirac singular representation.

Another feature of the single crystal case is that the boundary planes between regions of activation of single (the flat sectors) and double (the vertex sectors) slip plane traces differ from the ideally plastic boundary planes of RICE (1987) by an angle of order $1/n$ for large n. Even for small n the ranges of some of the sectors are very small [flat sectors (3) (5)]. Although the ranges of the other two flat sectors [(1) and (7)] do not vanish at large n, their stress states correspond to that of their adjacent vertices [(2) and (8), respectively].

Many other examples of HRR fields in cracked crystals could be studied with the general method presented here, simply by using different sets of parameters characterizing different yield surfaces. Also, the isotropic case could be solved as the limit of a many-sided polygon confined inside the unit circle defining its yield surface, analogous to the isotropic mode III case discussed by RICE and SAEEDVAFA (1988).

ACKNOWLEDGEMENT

This study was supported by the Office of Naval Research under contract N00014-85-K-0405 with Harvard University, and by the NSF Materials Research Laboratory at Harvard.

REFERENCES

HILL, R. 1967 *J. Mech. Phys. Solids* **15**, 79.
HUTCHINSON, J. W. 1968 *J. Mech. Phys. Solids* **16**, 13.
RICE, J. R. 1973 *J. Mech. Phys. Solids* **21**, 63.
RICE, J. R. 1987 *Mech. Mater.* **6**, 714.
RICE, J. R. 1988 *J. Elasticity* **20**, 131.
RICE, J. R. and ROSENGREN, G. F. 1968 *J. Mech. Phys. Solids* **16**, 1.
RICE, J. R. and NIKOLIC, R. 1985 *J. Mech. Phys. Solids* **33**, 595.
RICE, J. R. and SAEEDVAFA, M. 1988 *J. Mech. Phys. Solids* **36**, 189.
RICE, J. R., HAWK, D. E. and ASARO, R. J. 1989 Crack tip fields in ductile crystals. *Int. J. Fracture*, in press.